Unfried, Kerstin; Kis-Katos, Krisztina; Poser, Tilman

Working Paper

Water Scarcity and Social Conflict

IZA Discussion Papers, No. 14707

Provided in Cooperation with:
IZA – Institute of Labor Economics

Suggested Citation: Unfried, Kerstin; Kis-Katos, Krisztina; Poser, Tilman (2021) : Water Scarcity and Social Conflict, IZA Discussion Papers, No. 14707, Institute of Labor Economics (IZA), Bonn

This Version is available at:
https://hdl.handle.net/10419/245758

I Z A Institute
of Labor Economics
Initiated by Deutsche Post Foundation

DISCUSSION PAPER SERIES

IZA DP No. 14707

Water Scarcity and Social Conflict

Kerstin Unfried
Krisztina Kis-Katos
Tilman Poser

SEPTEMBER 2021

I Z A Institute
of Labor Economics

Initiated by Deutsche Post Foundation

DISCUSSION PAPER SERIES

IZA DP No. 14707

Water Scarcity and Social Conflict

Kerstin Unfried
University of Göttingen

Krisztina Kis-Katos
University of Göttingen and IZA

Tilman Poser
University of Göttingen

SEPTEMBER 2021

ISSN: 2365-9793

IZA – Institute of Labor Economics

Schaumburg-Lippe-Straße 5–9
53113 Bonn, Germany

Phone: +49-228-3894-0
Email: publications@iza.org

www.iza.org

ABSTRACT

Water Scarcity and Social Conflict*

Climate change and the increasing demand of water intensify the global water cycle, altering the distribution of water in space and time. This is expected to result in wet areas getting wetter and dry areas getting drier (Pan et al., 2015). As water is key to life, water scarcity is likely to provoke conflict. Using grid-cell data for Africa and central America over the years of 2002 to 2017, we establish a causal empirical link between the likelihood of local conflict and water mass declines. We measure water mass anomalies based on changes in Earth's gravity field recorded by GRACE and link them to social conflict events recorded in the SCAD data. To account for potential endogeneity in the demand for water, we instrument water mass change by the interaction of the number of drought months per year with yearly global average temperature changes. Our results show that a one standard deviation decrease in local water mass that follows from droughts and an intensifying water cycle more than triple the local likelihood of social conflict. Access to groundwater and surface water helps to mitigate these effects substantially. Water demand factors contribute to a quicker depletion of water mass in case of drought shocks, but do not intensify the link between water decline and conflict itself.

JEL Classification: D74, Q25, Q54
Keywords: social conflict, water scarcity, climate change

Corresponding author:
Krisztina Kis-Katos
Department of Economics
University of Göttingen
Platz der Göttinger Sieben 3
37073 Göttingen
Germany
E-mail: krisztina.kis-katos@uni-goettingen.de

* We would like to thank Stefan Döring, Andreas Fuchs, Robert Genthner, Markus Ludwig, Matthew Rudh and participants of the Conflict Dynamic workshop in 2020 for the helpful comments and discussions. All remaining errors are ours.

1 Introduction

The massive rise in the demand for blue water in the agricultural and industrial sector starting in the 1950s, together with continuous population growth, have amplified water scarcity in several parts of the world. Nowadays over-consumption of water is among the prime determinants of water scarcity (AghaKouchak et al., 2021). Global warming not only provokes the melting of ice resulting in an increase of sea level, but also raises evapotranspiration. As temperatures rise, the capacity of the atmosphere to hold water increases exponentially based on the Clausius-Clapeyron-relation. This leads to a redistribution of water from the earth into the atmosphere and to a rise in the frequency, duration, and intensity of extreme weather events (Huntington, 2006; Skliris et al., 2016). As a result, water crises are often listed among the largest global risks for the future (e.g., World Economic Forum, 2020).

The global prevalence of water-related conflicts and crises is already quite substantial, highlighting the conflict inducing potential of the competition over scarce resources as proposed by Homer-Dixon (1994). International disputes over the use of Nile water reappeared with the construction of the Grand Ethiopian Renaissance Dam between Ethiopia, Sudan and Egypt in 2020. In India, numerous inter-state conflicts over state-crossing rivers have erupted in the past five decades (Richards and Singh, 2002; CNA, 2017). Violent clashes between herders and farmers in Nigeria resulted in more than 1300 deaths in 2018 and led to the displacement of thousands of people.[1] In 2013, protests against the government arose in Senegal, when the capital was running out of water due to a damage in the water pipeline.[2]

Beyond triggering conflict onset in its own right, water also plays a critical role in exacerbating already existing tensions. Longer periods without rainfall, combined with bad water management and rapid population growth, caused a surge in thirst- and hunger-related deaths in Yemen as around half of the population struggled to fulfill their basic daily water needs.[3] The increase in grievance and inequality contributed to the onset

[1] Human Rights Watch (2018): Farmer-Herder Conflicts on the Rise in Africa, available at https://www.hrw.org/news/2018/08/06/farmer-herder-conflicts-rise-africa, accessed on 17.07.2020.

[2] Human Rights Watch (2013): Senegal seeks French, Chinese help as water crisis hits capital, available at https://www.reuters.com/article/us-senegal-water/senegal-seeks-french-chinese-help-as-water-crisis-hits-capital-idUSBRE98Q0MS20130927, accessed on 17.07.2020.

[3] Atlantic Council (2017): Running out of water: Conflict and water scarcity in Yemen and Syria, available at https://www.atlanticcouncil.org/blogs/menasource/running-out-of-water-conflict-and-water-scarcity-in-yemen-and-syria/, accessed on 17.07.2020.

of the civil war.[4] Additionally, water stress is used as leverage in conflicts. During the ongoing Syrian civil war, violent extremist groups have captured major dams in order to increase pressure on the government and coerce the local population (CNA, 2017). These examples and many others suggest a causal link between water shortage and conflict.

Although empirical evidence on the direct link between water scarcity and conflict is limited, a substantial literature documents the effects of climatic shocks on violent conflict (Miguel et al., 2004; Ciccone, 2011; Hsiang et al., 2013; Burke et al., 2015; Harari and La Ferrara, 2018). Yet, no consensus has been reached (Scheffran et al., 2012; Theisen et al., 2013). Given the wide range of the consequences of climate change, the controversial findings are not surprising. From the various channels through which climate change may trigger conflict, our paper focuses on increases in the local scarcity of water, which is an essential resource for human existence. Couttenier and Soubeyran (2014) use the Palmer drought index as a measure of exposure to water stress and find a weak positive link between droughts and civil war in Sub-Saharan Africa. Almer et al. (2017) show that droughts, measured by the standardized precipitation and evapotranspiration index (SPEI), lead to a higher likelihood of conflict in Sub-Saharan Africa using a grid cell-month panel. They conclude that droughts are especially conflict-increasing in cells with higher water demand (high agricultural activity) and low water supply.[5] These studies provide important insights on the short-term effects of economic shocks arising out of relatively low rainfall, yet they disregard the spatial dependence, the human impact and global climatic factors influencing local water availability. Therefore, it is unclear in how far these estimates capture the effect of climate change on conflict.

We contribute to this literature by providing empirical evidence on the direct link between reductions in water availability and conflict, and by focusing on the climate-change-induced intensification of the water cycle. Using a novel dataset that measures total water mass changes (at the surface as well as underground) at the grid-cell level, we are able to track water mass changes arising not only from rainfall anomalies but also from faster water outflows via evapotranspiration, an overuse of water resources, groundwater droughts, and changes in run-off. By that, we follow the suggestion by AghaKouchak et al. (2021) to regard water scarcity as a process of natural and human-induced changes rather than a product resulting out of natural changes only and ac-

[4] The Guardian (2015): Water scarcity in Yemen: the country's forgotten conflict, available at https://www.theguardian.com/global-development-professionals-network/2015/apr/02/water-scarcity-yemen-conflict, accessed on 17.07.2020.

[5] See Dell et al. (2014) for an overview of the literature.

knowledge the prevalence of water scarcity due to water over-consumption.

In this paper, we estimate the effect of a change in total available water mass within a grid-cell on the likelihood of local conflict. The simple correlation between water mass changes and conflict is likely to suffer from an omitted variable bias. For instance, local development dynamics—leading to economic and institutional change–can be expected to reduce the potential for conflict. At the same time, they can also lead to a quicker depletion of water reservoirs through intensifying water demand. This will lead to a negative correlation between water mass change and conflict, and bias the conflict inducing effects of water depletion downward. In order to establish a causal effect from reductions in available water on conflict, we instrument water mass change by the interaction of the number of drought months within each year derived from SPEI data (Croicu and Sundberg, 2015) with yearly changes in the average global temperature. Our IV strategy focuses on the intensification of the water cycle caused by climate change that alters water availability in space and time. Global warming leads to a faster evapotranspiration of water. This results in a loss of water into the atmosphere, and an increase in the intensity, duration and frequency of extreme weather events (Huntington, 2006; Skliris et al., 2016). Consequently, dry areas are expected to get even drier. Moreover, a drought of similar intensity can lead to larger losses of water mass on land. Our instrument captures this process. First, yearly average temperature changes account for the global effect of increased evapotranspiration on water loss on land. Second, we take the number of drought months within a year capturing the three most relevant aspects (duration, frequency, and intensity) of any particular extreme weather event at the local level. The combination of the two factors highlights that droughts will have stronger effects in warmer years as overall less water is available on land.

The instrumental variable approach rests on the assumption that the duration of a drought combined with global average temperature changes determines reductions in local water mass and affects conflict incidence only through the channel of water availability. As the water supply of a location is determined by groundwater storage, rainfall, runoff and underground water flows, rainfall anomalies are an excellent predictor of changes in water mass. Additionally, global temperature changes determine the overall loss of water mass into the atmosphere and ocean. We argue that after controlling for cell and country-year fixed effects and further geo-climatic controls that capture local anomalies in temperature and wind speed, the number of drought months interacted with average global temperature increase is exogenous to the likelihood of conflict. The geo-climatic controls help to exclude other channels of causation that may be correlated with localized drought occurrence, like excessive local temperatures that

make people more violence-prone (Hsiang et al., 2013).

Our analysis combines satellite data on water mass movements at a 1.0 grid-cell level, provided by the Gravity Recovery and Climate Experiment (GRACE) mission from US and German space agencies (NASA and DLR) (Wiese et al., 2018; Watkins et al., 2015; Landerer et al., 2020; Wiese et al., 2016) with geo-localized social conflict data from the Social Conflict Analysis Database (SCAD) (Salehyan et al., 2012). Changes in water mass are measured by deviations in the gravitation attraction of satellites circulating in Earth's orbit. We focus on social conflict as we believe that water scarcity directly provokes social disputes, and elaborate on the combined effect of water scarcity with already existing tensions by analyzing the effects on distinct types of conflict. Our dataset is a cell-year panel that consists out of 2,922 cells and covers Africa, Central America and the Caribbean, over the years 2002 to 2017.[6]

Apart from providing an estimate of the direct effect of water mass declines on conflict, we also identify which locations are the most affected ones based on time-invariant demand factors (capturing the presence of irrigation, mining activities and urbanization) and supply-side characteristics such as surface water and access to groundwater. Hence, our paper also speaks to the literature investigating the mediator role of water supply characteristics in driving conflict (such as Döring 2020 and Sarsons 2015). We also complement the literature by expanding the geographical scope of previous studies to include besides Africa also Latin America and by elaborating on regional heterogeneities.

The results show that a one standard deviation larger drought-induced reduction in the water mass within a cell more than triples the local likelihood of social conflict, increasing it from a baseline of 2% percent by 4.3 percentage points. The effect is substantially smaller in locations with access to groundwater. By contrast, we find no evidence for stronger conflict inducing effects of water mass decline in locations with higher water demand potential. However, as to be expected, the instrument of increasing drought intensity is linked to larger reductions in the local water mass in places with a potentially larger water demand due to irrigation, mining, or urbanization. Changes in water mass respond not only to current droughts but also to past droughts, emphasizing that studies that do not account for temporal dependencies may underestimate the magnitude of the effect of droughts on conflict.

[6]The sample is restricted to the years 2002 to 2017 because the GRACE data is starting in 2002 and the SCAD conflict data is only available until 2017.

2 Data, measurement and descriptives

2.1 Data and measurement

We combine data of water mass change at the grid-cell level with information on geo-referenced social conflict events to estimate the effect of water mass change on the likelihood of conflict. The analysis is at the cell-year level, whereby a cell refers to a resolution of 1.0 degrees (approximately 110 $\times$ 110 km). Our final panel dataset consists of 46,752 observations from 2,922 cells, located in 61 countries over the years 2002 to 2017. In our sample, the average yearly likelihood of a conflict is 2% per cell. The average cell experiences 3 drought months per year, and its mean yearly water mass change is about 0.52 centimeters of equivalent water thickness. Further descriptive statistics of the main variables are shown in table 1.

Table 1: Summary statistics

Variable	Mean	Sd	Min	Max	N
Social conflict	0.02	0.15	0.00	1.00	46752
No. of social conflicts	0.03	0.28	0.00	25.00	46752
No. of casualties	0.51	13.89	0.00	1890	46752
Δ Water mass	0.00	1.00	-9.74	28.82	46752
Drought months $\times$ Δ Global temp.	2.19	2.06	0.00	11.88	46752
Temperature	0.00	0.49	-3.27	3.06	46752
Meridional wind	0.00	0.60	-3.30	3.00	46752
Zonal wind	0.00	5.67	-20.21	21.21	46752
Surface water	0.38	0.49	0.00	1.00	46752
Groundwater access	0.22	0.41	0.00	1.00	46752
Irrigation	0.38	0.48	0.00	1.00	46752
Urbanization	0.01	0.04	0.00	0.42	46752
Mining	0.18	0.38	0.00	1.00	46752
State target conflict	0.01	0.10	0.00	1.00	46752
Non-state target conflict	0.01	0.11	0.00	1.00	46752
Resource conflict	0.001	0.04	0.00	1.00	46752
Political conflict	0.05	0.22	0.00	1.00	46752
Organized conflict	0.02	0.15	0.00	1.00	46752

Conflict measures

Our main dependent variable measures *Social conflict* incidence and indicates whether a cell experiences at least one conflict event in a certain year. We use conflict event information from the Social Conflict Analysis Database (SCAD) (version 3.3) that reports social conflict events over the years 1990 to 2017, covering all of Africa, Mexico, Central

America, and the Caribbean, with exact information on the location and time of each event (Salehyan et al., 2012). The dataset is unique in that it focuses on smaller scale social and local conflict events. It includes protests, riots, inter-communal conflict, and repression, among others. It excludes large-scale conflict like civil wars, organized rebellions, and international wars (Salehyan et al., 2012). The spatial distribution of the conflict events in the upper graph of figure 1 shows that social conflict is prevalent in different geographical areas of the sample, with one major conflict cluster in the North of Nigeria and another one in Tunisia.

Based on previous empirical and theoretical literature, we expect that the most likely form of conflict that is triggered by water scarcity is social conflict. The Homer-Dixon-model proposes three types of conflict that arise from resource scarcity: identity conflicts, social and political unrest as well as coups. Their empirical analysis shows that the latter is the least relevant with respect to the resource of water (Homer-Dixon, 1994). As identity conflicts as well as social and political unrest are included in SCAD, we rely on this dataset for our main analysis. Additionally, we also provide supportive evidence on other forms of conflict.

To investigate which types of conflict are especially driven by water scarcity, we classify conflict events based on definitions of the SCAD dataset. First, we divide conflict events by their target into *State target conflict*, capturing conflict events targeting the central government, and *Non-state target conflict* events that target other actors. Second, we limit our attention to *Resource conflict*, defined as such if food, water, subsistence, or environmental degradation were mentioned as the first, second or third most important source of tension. Additionally, we use two other conflict event databases, the Armed Conflict Location and Event Database (ACLED) and the Uppsala Conflict Data Program (UCDP), to measure conflict incidence at the cell-year level. Both datasets use somewhat different procedures to record conflict events and are especially useful to capture conflict that follows already existing tensions. The variable *Political conflict*, based on the ACLED data, captures political conflicts only, including riots, political protests, attacks against civilians and activities of militia and governments for Africa, Asia, Europe and Latin America (Raleigh et al., 2010). The alternative outcome variable *Organized conflict* is based on UCDP data and records organized violence at a larger scale for the whole world (Croicu and Sundberg, 2015). The analyses based on these two datasets serve as robustness checks, providing a general validation of our main results. Their advantage of larger geographical coverage comes at the cost of excluding smaller-scale social conflicts that are more likely to be directly caused by water scarcity.

Figure 1: Distribution of conflict events, droughts and water mass changes

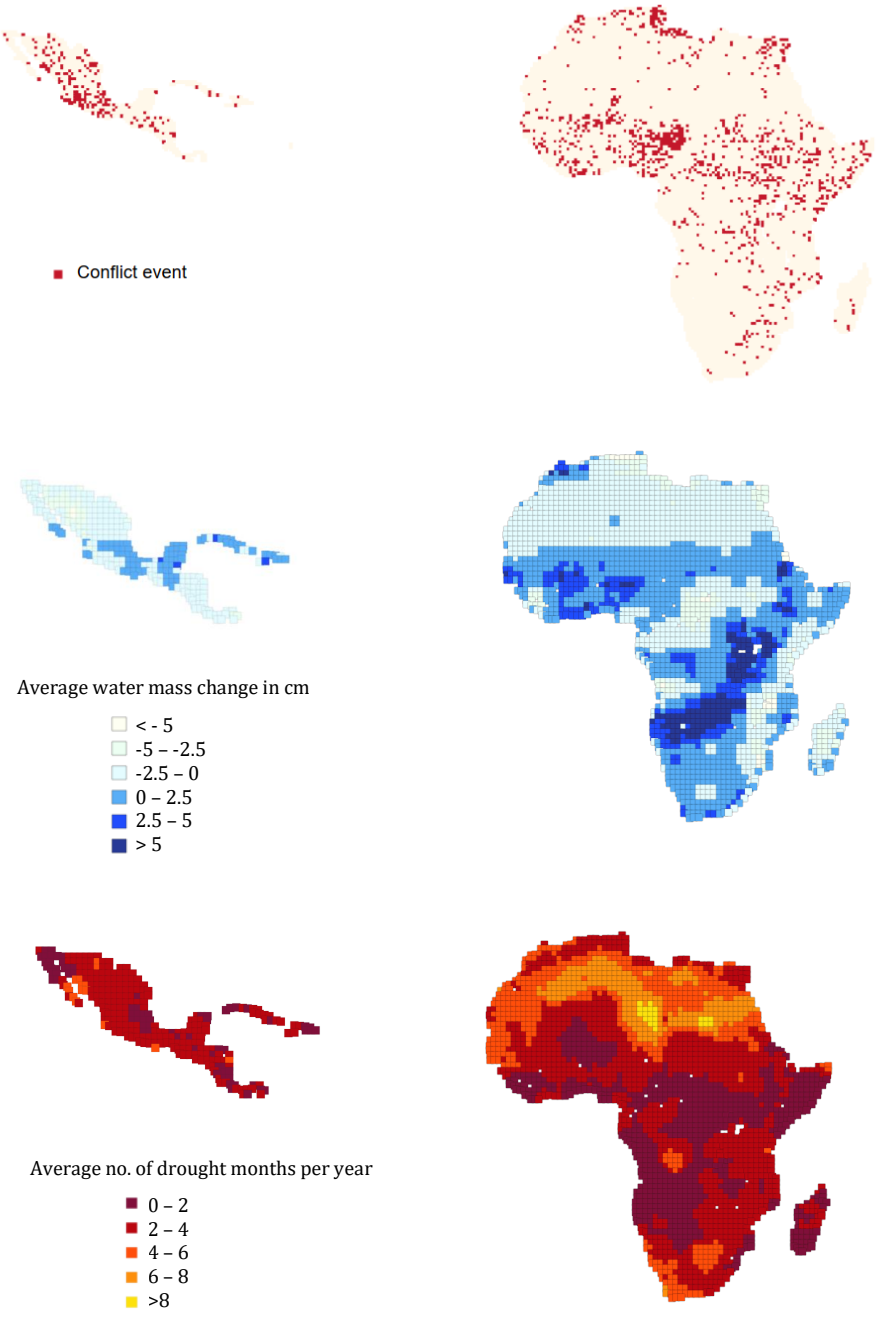

Note: The upper figure shows the location of conflict events during the sample period. Source: SCAD. The middle figure reports the average change in water mass over the sample period. Source: GRACE Tellus and FO, NASA and DLR. The lower figure reports the average number of months with SPEI values below -1 per year during the sample period 2002 to 2017. Source: SPEIbase.

Water mass change

Our main explanatory variable Δ *Water mass* captures the change of water mass per grid cell and year, expressed in standard deviations. Water mass incorporates all kinds of water, including soil moisture, groundwater as well as surface water like rivers and lakes. Hence, water mass change measures the change in total available water within a certain grid cell. We focus on changes in water mass instead of the level of water mass, because we believe that changes in water mass provide a better indicator for accessible fresh water availability. A major share of the total water mass on land is stored as groundwater deep underground. This water mass is less accessible for humans and would generate a false perception of water availability. In the long-run, the amount of water mass at a certain location depends on the speed and amount of water in- and outflows (Oki and Kanae, 2006). Moreover, we are interested in how the intensification of the water cycle caused by climate change affects the likelihood of conflict. To capture this accelerating process, our panel models focus on the dynamics in water mass changes. A more practical reason to focus on changes instead of levels is due to the format of the available geophysical data that can only detect changes but not levels of water mass.

To compute change in water mass, we rely on a novel data source that records water mass movements (but not levels) based on satellite data for the years 2002 to 2017. More specifically, we use the processed GRCTellus JPL Mascon monthly mass grid dataset (release 6) that is based on observations of global mass flux gathered by the Gravity Recovery and Climate Experiment (GRACE) mission from US and German space agencies (NASA and DLR) (Wiese et al., 2018; Watkins et al., 2015; Landerer et al., 2020; Wiese et al., 2016).

Water mass changes are measured by the small changes in the distance between two satellites that follow each other in orbit when circulating around the Earth. The small changes arise out of shifts in the Earth's gravity field. Less mass on Earth results in a weaker gravity field, whereas more mass leads to a stronger gravity. The underlying assumption of the measurement approach is that the only considerable mass that is changing on earth is water mass (Cooley and Landerer, 2019). The dataset has been cross-validated with other data sources of water mass changes at specific locations (Scanlon et al., 2016; Chambers and Bonin, 2012; Klosko et al., 2009). The Mascon processing procedure uses geophysical constraints on the regional level to filter out noise and does not need further de-striping algorithms or smoothing, like traditional spherical harmonic gravity solutions do (Watkins et al., 2015).[7] Additionally, a Coastal

[7] A detailed description of the processing procedure is described in Watkins et al. (2015) and

Resolution Improvement (CRI) filter is applied to the data. The processed data records water mass anomalies of each month with respect to the time average of 2004 to 2009 at the 1.0 degree grid-cell level in equivalent water mass thickness in centimeters. The native resolution of measurement is at the 3 degree grid level. Gain factors derived from a CLM hydrological model are applied to the data to extrapolate the GRACE estimates from their effective spatial resolution to the finer spatial scale. To account for the native resolution, we cluster standard errors at that level to allow for the interdependence of measurement and rerun the analysis on the 3 degree grid cell level as a robustness check.

We aggregate the data on a yearly level by taking the average over all months in a year. The middle graph in figure 1 depicts the spatial distribution of the average changes in water mass in our sample. It shows that the decline in water mass visibly varies in our sample area, and that there are geographical clusters. The Northern part of central America and the Sahel-region experienced strong water declines, whereas in the middle and south of Africa water mass increased on average.

Drought months $\times$ Δ Global temperature

In our empirical analysis, we instrument the change in water mass by the interaction of the number of drought months per year with the average yearly global temperature increase. We base our drought indicator on the standardized precipitation and evapotranspiration index from the SPEIbase (version 2.5), computed at a 3-month scale. The SPEIbase reports monthly information on drought conditions at a 0.5 grid cell resolution. It measures precipitation anomalies by a standardized z-score that is based on monthly precipitation and potential evapotranspiration information provided by the Climatic Research Unit of the University of East Anglia (Vicente-Serrano et al., 2010). We define a month to be affected by a drought if the SPEI value is below -1 in a given grid cell and count the number of months with drought per year. This is in contrast with the previous literature (e.g., Almer et al., 2017; Harari and La Ferrara, 2018) that generally measures droughts by the average value of the SPEI. The advantage of our approach is that it takes the length of droughts into account explicitly and allows us to focus on droughts of sufficient severity. We test the sensitivity of our results to other SPEI thresholds in a robustness check. The spatial distribution of average drought months per year is shown in the lower graph of figure 1. During our sample period, central Africa has been less affected by droughts than North Africa where droughts were pervasive, with an average of more than 6 drought months per year. The majority of cells

Wiese et al. (2016).

located in central America experienced on average 2 to 4 drought months per year.

Information on the change in global yearly temperature is provided by the Global Historical Climatology Network-Monthly (GHCN-M) data set and International Comprehensive Ocean-Atmosphere Data Set (ICOADS). Δ *Global temperature* gives the yearly increase in temperature in degree Celsius relative to the average temperature measured between 1910 and 2000. The increase ranges between 0.54 (in 2008) to 0.99 (in 2016) degree Celsius.

Demand and supply factors

In the heterogeneity analysis, we investigate differential effects of water mass change on conflict by interacting them with time-invariant measures of water supply and demand. As supply factors we consider the availability of surface water and access to groundwater. We define a cell to hold *Surface water* if a river or lake is located within the respective cell. Information on the geographical location of rivers and lakes is taken from the river and lake centerlines map (version 4.1) provided by Natural Earth (2020). The ease of access to underground water sources crucially depends on two factors, the local abundance of groundwater and its general reachability. Therefore, our *Groundwater access* indicator combines information on the quantity of groundwater storage within the area and the depth at which groundwater can be found. We define a cell as having access to groundwater if it is part of a high groundwater storage area and at the same time the depth to groundwater is low. Information on groundwater storage is taken from the Groundwater Resources of the World database (WHY map BGR version 1.0) provided by the World-wide Hydrogeological Mapping and Assessment Programme. It classifies groundwater sources based on the geological components of the aquifer in three categories: major groundwater basin, complex hydrological structure, and shallow and local aquifer. Based on this information, we define a cell as having high groundwater storage if its groundwater source is classified as a part of a major groundwater basin (Richts et al., 2011). Information on the depth until reaching groundwater is taken from Fan et al. (2013). Their map gives water table depths in meters below land surface at a 1 km grid resolution. The map is constructed by integrating over 1 million data points measured at well sites into a groundwater model. We aggregate the information to a 1.0 degree resolution and divide locations along the median (approximately 25 mbgl). Based on these definitions, around 25% of our sample has access to abundant groundwater.

With around 70% of total water use, agriculture is the far biggest consumer of water in the world (Siebert et al., 2013). In agriculture, water is mainly used to irrigate crops.

Therefore, we operationalize agricultural water demand by identifying areas that are irrigated. We base our measure on the global irrigated area map (GIAM) provided by the International Water Management Institute (IWMI) (Thenkabail et al., 2009). Using satellite images, the map identifies irrigated areas in 2000 at a 10 km resolution. Based on these data, we construct the indicator variable *Irrigation* that takes the value of one if an irrigated area is located in a cell. 37% of the grid cells in our sample have irrigated areas.

Mining is another sector that can heavily rely on water. Water is needed for a broad range of activities in the mining process such as mineral processing and dust suppression (Garner et al., 2012). We use the major mineral deposits of the world dataset provided by U.S. Geological Survey (Schulz and Briskey, 2005) in combination with the global-scale data set of mining areas to identify locations with mining potential (Maus et al., 2020). The USGS dataset provides the geographical location of deposits of major non-fuel mineral commodities whereas the latter dataset identifies mining areas using satellite images. Based on this information, we define a cell as potentially active in *Mining* if at least one major known mineral deposit or a mining area is present in the cell. According to this definition, 18% of the grid cells in our sample have mining potential.

Water consumption increases with population size. Therefore, as a third water demand factor, we distinguish grid cells based on their population size. We rely on the Urban Extents Grid database provided by the Socioeconomic Data and Application Center (SEDAC) that differentiates urban and rural areas based on population size, settlement areas, and the presence of nighttime lights. On a 30 arc second resolution, urban areas are identified by connected lighted cells or settlement points for which the total population is greater than 5,000 persons (SEDAC, 2011; Balk et al., 2006). We aggregate the data to the 1.0 degree resolution by measuring the share of urbanization per cell. The variable is called *Urbanization*.

Atmospheric factors

Among the atmospheric factors, we control for *Temperature* and two dimensions of wind speed. We rely on monthly averages provided by the NCEP/NCAR 40-year reanalysis project from the Physical Science Laboratory (PSL) that processes daily data on wind speed and temperature from the National Center for Environmental Prediction (NOAA) (Kalnay et al., 1996). Temperature data are reported in degree Celsius, whereas wind speed is measured as *Zonal wind velocity* and *Meridional wind velocity*. Zonal wind velocity measures the wind speed in meter per second in the west-east direction, whereas meridional wind velocity captures wind speed in north-south direc-

tion. We separate wind speed by direction because the direction of the wind flows is associated with different meteorological conditions. Meridional flows tend to go along with extreme weather events, whereas zonal wind is connected to quiet weather conditions (Milrad, 2017). We aggregate the data to the spatial resolution of 1.0 degrees and to a yearly level by taking averages. We include these control variables in form of deviations from the sample mean.

2.2 Descriptive trends

As water is a renewable resource, the total water mass on land, in oceans and in the atmosphere is constant over time. Yet, the speed of water movements along the water cycle can change, for instance due to global warming or human activity. Since we focus only on water mass on land, average declines in the local water mass are possible and arise from a redistribution of water in space due to the global water cycle. Global warming raises water vapor, such that more water evaporates and is stored in the atmosphere. The latent heat and condensation affect energy flows of the climatic system, resulting in a higher frequency, intensity and duration of extreme weather events (Allan, 2012; Pan et al., 2015). Moreover, temperature increases provoke the melting of ice sheets and glaciers, raising the water mass in the oceans. Overall, climate change is expected to result in wet areas getting wetter and dry areas getting drier (Huntington, 2010; Oki and Kanae, 2006; Pan et al., 2015).

Human activities can increase the speed of water in- and outflows (Kuchment, 2004). The withdrawal of groundwater as drinking source or for irrigation can result in groundwater depletion if more water mass is withdrawn than recharged (Vörösmarty and Sahagian, 2000). This often results in a reduction of the terrestrial water mass as slowly moving groundwater evaporates partly on the surface. Irrigation in river basins or the construction of artificial water reservoirs shapes the ratio of run-off to evapotranspiration, resulting in less water inflow in downstream areas (Kuchment, 2004). Other human activities also alter the water cycle (see e.g., Vörösmarty and Sahagian, 2000).

The novel dataset on water mass change enables us to observe how water movements change over time. The left panel of figure 2 presents the average water mass change in equivalent water mass thickness in centimeters over the sample period of 2002 to 2017 (compared to the time average of 2004 to 2009). It reports average water mass change for the whole world (measured on terrestrial land mass) as well as for the two continents included in our conflict data sample, Africa and Central America combined with Mexico. The right panel of figure 2 shows how the standard deviation of water

Figure 2: Change of water mass over time

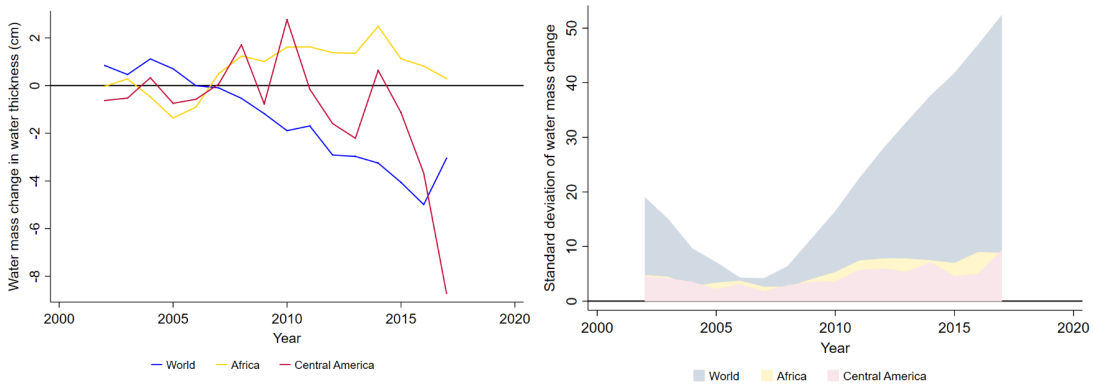

Note: The figure reports the average water mass change over the years 2002–2017. Water includes all kinds of surface and underground water. Source: GRACE Tellus and FO, Nasa and DLR.

change developed over time.

On a global level, the data depicts the expected patterns associated with climate change and the increased demand for water. On the one hand, the change in water mass follows a strongly negative trend, with larger water mass declines in later years. These declines reflect the loss of terrestrial water to oceans through glacier melting and into the atmosphere through increased evapotranspiration caused by global warming and water over-consumption (Sasgen et al., 2020; Dessler et al., 2008; Brutsaert, 2017). On the other hand, the spatial variation in water mass change has substantially increased since 2006, reflecting the more unequal distribution of rainfall in the world. This highlights that localized water scarcity is likely to become more prevalent in the future.

Within our chosen geographical area, we see two distinct trends. Water mass change in central America follows a negative trend that is broadly similar to the global one. However, it strongly surpasses the global declines by the end of our time period. By contrast, average water mass in Africa has increased over the last decade. It is also evident that some locations are more affected by water decline than others. For instance, the water mass increases measured in Africa are driven by water mass gains in the South of Africa. At the same time, the Sahel zone experienced a water mass loss. On both continents, the variation of water mass change has substantially increased over time.

The following empirical analysis will utilize this spatial and temporal variation of water mass change to infer the effect of shifts in water mass on social conflict. Moreover, it

will isolate the weather induced variations in water availability by predicting Δ *Water mass* by the interaction between localized drought occurrence and global temperature increases. Figure 3 shows the average temporal dynamics of this instrument (number of drought months per year combined with global average temperature increases) for the world, Africa and central America. Additionally, it shows the yearly global temperature increases in degree Celsius in the background. For both factors, we see a global increase over time, confirming the general patterns expected by climate change.

Figure 3: Temporal dynamics of temperature change and drought months

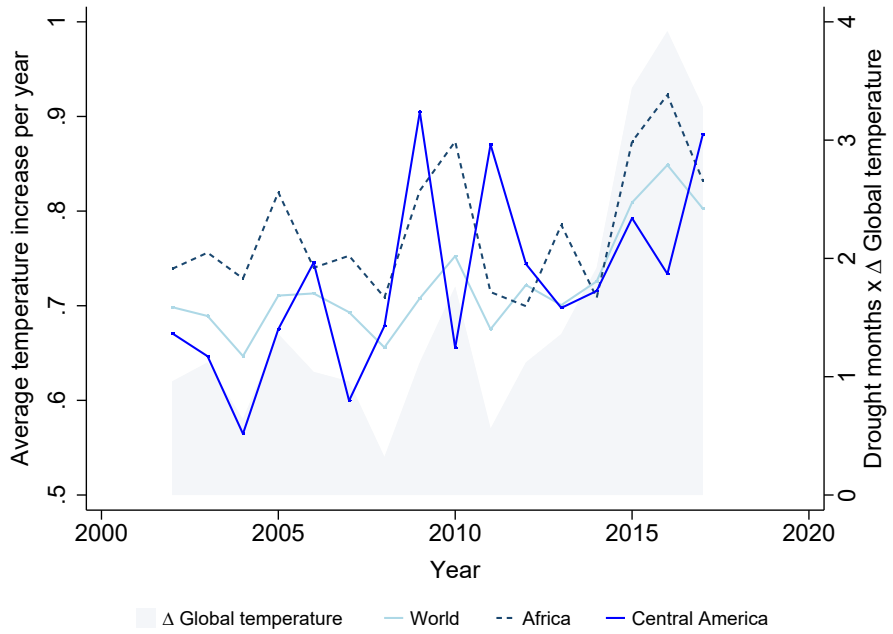

Note: The figure reports the number of drought months per year interacted with global temperature increases over the time period 2002-2017 for the world and the two analysed continents. A drought month is defined by SPEI values below −1. Source: SPEIbase. The colored background area presents the average yearly increase in global temperature in degree Celsius. Source: GHCN-M, ICOADS.

3 Empirical strategy

In order to estimate a causal effect of change in water mass on conflict incidence, we apply an instrumental variable approach, using the temporal and spatial variation of negative rainfall shocks combined with global temperature changes. Our baseline esti-

mation model is defined as follows:

$$Social\ conflict_{ict} = \beta\, \Delta Water\ mass_{ict} + \mathbf{X}'_{ict}\theta + \alpha_{ct} + \mu_i + \epsilon_{ict}, \quad (1)$$

where $Social\ conflict_{ict}$ is an indicator variable that takes the value of one if a social conflict event occurred in year t and grid cell i (1°), located in country c. Δ $Water\ mass_{ict}$ measures the change of water mass in standard deviations in the respective year and cell. Throughout all estimations, β is the coefficient of interest, measuring the effect of local water mass change on the likelihood of conflict. $\mathbf{X}_{ict}$ describes a vector of control variables that includes temperature and wind speed. Standard errors are robust and clustered at the 3° grid-cell level to account for the native resolution of measurement of water mass change. The regressions include cell fixed effects, μ_i, combined with country-year fixed effects, α_{ct}. Cell fixed effects control for all time invariant differences between locations, absorbing spatial differences in average changes of water mass and the propensity to experience conflict. Country-year fixed effects absorb the country-wise effects of all major shocks, such as economic crises or El Niño years. Additionally, they also account for more idiosyncratic yearly variation in the national water management system, climatic conditions, as well as of country-specific political, social, and economic shocks.

A remaining endogeneity problem arises as local changes in water mass are not random but also reflect variation in water demand by the local population. For instance, a massive immigrant inflow may increase local water demand, resulting in a decline of water mass by accelerating the speed of water outflows, and at the same time provoke conflict (Brückner, 2010). If we are not able to fully control for the extent of the local immigration shock, this would lead to a spurious negative correlation between water availability and conflict. Alternatively, positive income shocks due to an increase in commodity prices may lead to a higher demand for water (due to more irrigation) but also increase the opportunity costs of social unrest (Dube and Vargas, 2013), potentially biasing a true negative relationship between changing water availability and conflict towards zero. In particular, we regard economic development as a potential omitted variable that biases our estimates downwards. For many economic activities water is necessary and utilized. Hence, economic activity often strategically takes place in areas with abundant water supply or even provides water supply by redirecting water mass from other locations. Moreover, with economic development access to groundwater is likelier to be established. If more water is withdrawn than recharged, this would result in a water mass decline at the certain location. At the same time economic development

reduces the likelihood of conflict due to higher opportunity costs to fighting (Hodler and Raschky, 2014). Also other economic activities such as deforestation, built-up area expansion, air pollution, and agriculture shape the water cycle and are connected to economic development.

Lastly, a systematic measurement error could potentially provoke endogeneity problems. Water mass changes are measured by changes in the gravity field. Apart from water mass also larger natural disasters such as earthquakes of magnitude larger than 8.8 and volcanic eruptions can cause changes in the power of attraction, which is measured by GRACE. These concerns are in our view of lesser importance as such events only account for tiny changes in the water mass (De Viron et al., 2008; Han et al., 2006). But if natural disasters are a determinant for the probability of conflict, this would bias our estimates downward. There is some evidence for that (Xu et al., 2016). Another systematic measurement error could arise in the data processing of the satellite measures.

To deal with these endogeneity concerns, we instrument the change in water mass by a measure of exogenous declines in local water availability: the interaction of the number of drought months in the respective year and cell with yearly global average temperature increases. Our second stage regression remains as described by equation (1), but it is extended by a first stage that takes the following form:

$$\Delta \, Water \; mass_{ict} \quad = \quad \gamma \, Drought \; months_{ict} \times \Delta Global \; temp_t + \mathbf{X}'_{ict}\theta + \alpha_{ct} + \mu_i + \epsilon_{ict}, \quad (2)$$

and includes both cell fixed effects, μ_i, and year or country-year effects, α_{ct}.

The empirical strategy rests on the assumption that the duration of droughts in combination with global warming jointly determine the change in local water mass and affect the incidence of violent conflict only through this channel. Apart from groundwater storage, runoff and underground water flows, rainfall is the main determinant of local water supply. Global temperatures determine the rate of evapotranspiration and the likelihood, intensity, and duration of extreme weather events. Hence, the combination of rainfall anomalies at the local level together with changes in global temperature provide an excellent instrument for water mass change. Rainfall anomalies have been widely used in the conflict literature as an instrument for economic shocks in developing countries (Miguel et al., 2004; Ciccone, 2011; Harari and La Ferrara, 2018). These studies argue that in agriculture-based economies, the lack of rainfall reduces crop yields (because of water scarcity), triggering an economic shock. Our approach follows this argument, yet we also emphasize that a change in water availability may affect conflict directly as well, for instance because of arising water right disputes or

civil unrest. Our instrument provides a local average treatment effect (LATE) by isolating the effect of water mass change that is induced by exogenous drought shocks together with their intensifying effect on local water mass fluctuations due to climate change.

We include a vector of atmospheric factors as controls to account for potential omitted variable biases. For instance, heat may trigger aggressive behavior and shape decision making (Anderson, 1989; Almås et al., 2019; Anderson et al., 2000), while at the same time, it is likely to accompany droughts. Heavy wind speed can disrupt economic activities (Nelson, 2010; Slettebak, 2012), while being correlated with the occurrence of precipitation (Waliser and Guan, 2017). If rainfall anomalies in interaction with global temperature are closely linked to such atmospheric factors, we falsely attribute their effect to our instrumented endogenous variable. By that, we would overestimate the effect of water scarcity on conflict. Therefore, we include *Temperature*, *Zonal* and *Meridional wind speed* as control variables in both stages of our regressions. Additionally, climatic conditions may restrict the mobility of fighters, for instance through floods. However, as our measure concentrates on droughts, we expect that our approach is unaffected by such dynamics.

We argue that conditional on cell and country-year fixed effects and local geo-climatic controls, the number of drought months interacted with global temperature change is exogenous to conflict incidence. Whereas the number of rainfall anomalies varies across climatic zones and with geographical factors like terrain or elevation, and the local susceptibility to climatic change (which potentially also affects the likelihood of conflict, see Breckner and Sunde 2019), the spatial and temporal distribution of rainfall deviations within a grid cell and year is as good as random. Note that the average effect of global warming on conflict is captured by the country-specific year fixed effects in our model.

A remaining threat to the exclusion restriction of our instrument may also arise from air pollution, which can shut-off precipitation under certain circumstances (Rosenfeld, 2000). If air pollution correlates with the likelihood of conflict, our estimates may be biased. To our knowledge, there is no empirical evidence that suggests that air pollution provokes conflict directly, but there may be a correlation between pollution and conflict through the connection of air pollution to economic activity. In a robustness check we therefore control for fine particulate matter density in the air.

4 Results

4.1 Baseline results

Table 2 reports our baseline results from regressing the incidence of social conflict on the change of water mass, conditional on fixed effects. Columns 1 and 2 show OLS estimates, whereas columns 3 and 4 present our preferred specifications in which the change in water mass is instrumented by the number of drought months interacted with average changes in global temperature in the respective year. Columns 5 shows the reduced form estimates whereas columns 6 and 7 document the corresponding first stage results. All models include cell and country-year fixed effects. Two models are shown, one without and the other with additional atmospheric control variables.

The OLS results in columns 1 and 2 show no significant correlation between a change in water mass and conflict after controlling for time-invariant cell characteristics and country-wide temporal shocks. The OLS results are most likely biased though (as outlined in section 3), as water mass change responds strongly to economic and political factors influencing water demand and conflict at the same time. If omitted local development dynamics are negatively correlated not only with conflict but also with water mass change, this will bias a possible negative correlation between water mass change and conflict towards zero.

Table 2: Baseline results

Dependent variable:			**Social conflict**			**Δ Water mass**	
Model:	OLS		IV: Second stage		Reduced form	IV: First stage	
	(1)	(2)	(3)	(4)	(5)	(6)	(7)
Δ Water mass	0.001	0.001	-0.043*	-0.047*			
	(0.001)	(0.001)	(0.024)	(0.026)			
Drought months × Δ Global temp.					0.001*	-0.031***	-0.028***
					(0.001)	(0.006)	(0.006)
Temperature		0.001		-0.005	0.001		-0.126***
		(0.002)		(0.004)	(0.002)		(0.027)
Meridional wind		-0.001		-0.004	-0.001		-0.064**
		(0.003)		(0.003)	(0.003)		(0.021)
Zonal wind		-0.001**		-0.001*	-0.001**		0.003
		(0.001)		(0.001)	(0.001)		(0.003)
Observations	46,752	46,752	46,752	46,752	46,752	46,752	46,752
Kleibergen-Paap F stat.			28.13	23.36			
Stock-Yogo critical value (10%)			16.38	16.38			
Fixed effects	Yes	Yes	Yes	Yes	Yes	Yes	Yes

Note: The table reports OLS and IV coefficient estimates of an indicator variable for social conflict on the change of water mass within each cell. Models include cell and country-year fixed effects. Robust standard errors are clustered at the 3 degree cell level. The mean of the dependent variable is 0.02. *** p<0.01, ** p<0.05, * p<0.1

We address the potential endogeneity concern by instrumenting the change of water mass by the number of drought months per cell and year in combination with changes in the average global temperature. Our reduced form estimates in column 5 replicate the findings of the previous literature, linking our drought instrument to a higher likelihood of social conflict. When implementing this instrument in a two-stage procedure, we see a highly significant effect of our instrument on the change in the local water mass in the first stage (columns 6 and 7). The significant effect and the Kleinbergen-Paap F-statistic (above 20) confirm the relevance of our instrument. Conditional on cell and country-year fixed effects, a further drought month is estimated to induce a 0.031 standard deviations stronger decline in water mass. The effect is significant at the 1% level. The more restrictive model, including control variables (column 7), factors out other climatic shocks. In this specification, the effect of drought months on water mass change decreases only slightly to 0.028 standard deviations, whereas the relationship between water mass change and atmospheric conditions is as expected. Higher temperatures go along with larger decreases in water mass. Zonal wind speed (measuring wind flows from west to east or vice versa) is not related to changes in the water mass, but meridional velocity, which is associated with extreme weather events (Milrad, 2017), is linked to water mass decline.

At the second stage, the IV results show a negative and significant relationship between shifts in the water mass and local conflict incidence (in columns 3 and 4). A one standard deviation larger decrease in the local water mass increases the likelihood of social conflict by 4.3 percentage points, or 4.7 percentage points once atmospheric factors have been controlled for. With an average yearly likelihood of conflict of 2%, the effect is substantial as a one standard deviation lower change in water mass more than triples the local likelihood of conflict. Note that a one standard deviation larger decline in water mass represents a decline of 5.7 cm thickness. This means on average at a 1 degree grid cell level a loss of (5.7 cm $\times$ 110 km $\times$ 110 km =) 0,6897 km^3 water per year, which is sizeable.

We conclude that changes in water availability, induced by exogenous variation in the local duration of drought, shape the likelihood of conflict. We find no correlation between change in water mass and conflict in the OLS setting, indicating that the OLS estimates are biased. This suggests that increases in water demand go along with factors reducing the likelihood of conflict. For instance, water depletion is likely to increase during economic upturns if they go along with increased water demand. At the same time, economic growth increases the opportunity costs to fight. This induces a positive correlation between conflict and water mass change, biasing the conflict inducing effect

of a declining water mass downward.

An alternative interpretation of the results is that drought-induced changes in water mass have a different effect as compared to changes in water mass caused by other factors such as over-consumption. We would expect that water mass changes from other natural factors, e.g., drought shocks in neighboring areas resulting in less run-off, are likely to provoke the same effect. Water mass changes caused by human activity potentially provoke different reactions as the attribution of blame changes. Therefore, we will explore the differential effects by water demand and supply factors next. In what follows, we will only focus on our IV model from column 3 of table 2 that includes both cell and country-year fixed effects. As the atmospheric control variables reduce the power of our instrument somewhat but at the same time lead to a slight increase in our estimation coefficients, excluding these controls results in more conservative estimates.

4.2 Heterogeneous effects by supply and demand factors

Water scarcity arises when local water demand exceeds the current water supply. It can result out of a higher demand for water, a lower supply of water or a combination of both. Around the globe, water supply varies strongly. Whereas some regions are equipped with large and persistent groundwater storage, reducing their susceptibility to rainfall shocks and water demand shocks, other regions lack such a buffer and are more vulnerable to shifts in water demand or supply. Yet, even if groundwater storage is high, it may be unreachable for the local population if it is situated deep underground. Hence, we expect heterogeneous effects of changes in water mass on conflict depending on the local accessibility and the locally available amount of water.

Columns 1 and 2 in table 3 present the heterogeneous effects of water mass change on conflict by supply factors. We investigate the heterogeneity by estimating the differential effect of drought in water-rich as compared to water-poor locations. For this purpose, we include an interaction term of water mass change and the respective time-invariant supply factor in the regression as second, potentially endogenous, explanatory variable. To deal with the additionally arising endogeneity, we add the interaction of our instrument with the respective supply factor as a further instrumental variable to both first stages. Column 1 presents results differentiated by the availability of surface water and column 2 by access to groundwater. First stage results show that drought months reduce the measured water mass substantially more in places with surface water compared to locations without surface water (column 1). We find no significant difference in the effect of drought on total water mass change in places with a better

or worse access to groundwater (column 2). Taken together, the two sets of results indicate that water mass at the surface varies more strongly with drought than the one underground.

The second stage results show a significant difference in the effect of water mass change on conflict depending on the presence of surface water and groundwater. In cells without surface water a one standard deviation decrease in water mass increases the likelihood of conflict by 6.9 percentage points. This effect is reduced by 4.9 percentage points in cells with surface water. In cells without an easy access to groundwater, a standard deviation larger decrease in water mass increases the likelihood of conflict by 5.4 percentage points. With accessible groundwater, this effect reduces by 4.2 percentage points. The sum of these two coefficients shows no significant effect of climate-induced water mass changes in regions with sufficient water storage. These results confirm that local access to abundant water can act as a buffer to climatic shocks, substantially reducing the effect of drought shocks on conflict.

Like water supply, water demand is also distributed unevenly in space. Accounting for around 70% of the total water demand, agriculture is the main water consumer in the world (Otto and Schleifer, 2020). Additionally, water demand is higher in more populated areas and in locations where water-intensive industries are located such as mining and energy production (Otto and Schleifer, 2020). The pivotal role of water in these areas leads us to hypothesize that the effect of water mass change on conflict is stronger in locations with higher water demand compared to locations with lower water demand.

We analyze the heterogeneous effects by water demand focusing on the wide-spread prevalence of irrigation, the potential presence of mining, and the extent of urbanization. The demand factors enter the regression in the form of interactions, similar to the supply factors above. Column 3 in table 3 presents the results for irrigation, column 4 for mining, whereas column 5 shows the heterogeneous effects by urbanization. In the first stages, we estimate a stronger reduction in water mass in the aftermath of drought in areas with potentially higher water demand. These results indicate that during drought even more water is consumed in economically more advanced rural as well as in more urbanized areas.

Surprisingly, the second stage results show a weaker increase in conflict with declines in water availability in irrigated areas compared to non-irrigated areas (column 3). We find no differential effects by mining activities or urbanization. A potential explanation of the weaker effect in irrigated areas is the strategic location of irrigated agricul-

Table 3: Heterogeneous effects by water demand and supply factors

Dependent variable:	**Social conflict**				
Interacted factor:	**Surface water**	**Groundw. access**	**Irrigation**	**Mining**	**Urban-ization**
Model:	IV: Second stage				
	(1)	(2)	(3)	(4)	(5)
Δ Water mass	-0.069**	-0.054**	-0.065**	-0.049*	-0.049**
	(0.028)	(0.024)	(0.029)	(0.026)	(0.025)
× Interacted factor	0.049***	0.042**	0.039*	0.017	0.248
	(0.017)	(0.021)	(0.021)	(0.015)	(0.175)
Dependent variable:	**Δ Water mass**				
Model:	IV: First stage				
Drought months × Δ Global Temp	-0.022***	-0.031***	-0.026***	-0.027***	-0.028***
	(0.005)	(0.006)	(0.007)	(0.006)	(0.006)
× Interacted factor	-0.027**	-0.002	-0.016*	-0.025*	-0.243*
	(0.009)	(0.010)	(0.008)	(0.011)	(0.122)
Dependent variable:	**Δ Water mass change × Interacted factor**				
Model:	IV: First stage				
Drought months × Δ Global Temp	0.013***	0.004	0.007*	0.009***	0.001**
	(0.003)	(0.002)	(0.003)	(0.002)	(0.000)
× Interacted factor	-0.089***	-0.059***	-0.068***	-0.110***	-0.102***
	(0.012)	(0.014)	(0.009)	(0.014)	(0.021)
Observations	46,752	46,752	46,752	46,752	46,752
Kleibergen-Paap F stat	14.51	14.26	11.60	13.38	12.77
Stock-Yogo critical value (10%)	7.03	7.03	7.03	7.03	7.03
Fixed effects	Yes	Yes	Yes	Yes	Yes

Note: The table reports IV coefficient estimates of the incidence of social conflict within each cell on the change of water mass and interactions with supply and demand side factors. The interactions of water change and the various supply and demand factors are instrumented by drought months combined with global average temperature changes and the interaction of it with the respective factor. Surface water measures the presence of rivers or lakes within the cell; groundwater access indicates low depth to groundwater and high groundwater storage; irrigation indicates the presence of any irrigated area within the cell; mining indicates the presence of major mineral deposits; urban marks the share of urban areas in the cell. The models include cell and country-year fixed effects. Standard errors are clustered at the 3 degree cell level. The mean of the dependent variable is 0.02. *** $p<0.01$, ** $p<0.05$, * $p<0.1$

tural production in areas with groundwater access, which hampers a clean distinction between the effects of irrigation and groundwater access. Moreover, irrigation infrastructure can act as a buffer mitigating the climatic shocks on conflict (Gatti et al., 2021). Overall, the results do not confirm our hypothesis. They indicate that although water demand factors accelerate water scarcity, they do not intensify the effect of water mass change on conflict. Yet, the results indicate that in these areas there is a higher potential for water scarcity as in times of lower water mass inflow, water mass declines more strongly, potentially driven by water consumption that leads to higher water mass outflows.

4.3 Further heterogeneities

In our baseline estimation, we used a broad conflict measure that reports if any conflict event occurred in a given year and cell. In order to investigate whether water scarcity also affects the intensity of conflict, we run further regressions estimating the effects of water scarcity on the number of conflict events within a year and cell and on the number of casualties. The variables enter the regression in three forms: in levels, in a log-transformation using the inverse hyperbolic sine function as well as relying on a Poisson model for count data. The estimates shown in table 4 document a significant effect of water mass change on the number of conflicts but not on how deadly the conflicts are, captured by the number of casualties. Taken together the results show that water scarcity increases the likelihood of conflict events but has no effect on the intensity of fighting.

In our main analysis, we focus on social conflict based on the Homer-Dixon-model (1994). The model proposes that two types of conflict are likely to arise with water scarcity: migration-induced identity conflicts and social and political unrest due to economic deprivation. Social disputes between inhabitants are more likely when a resource that is necessary to survive becomes scarcer. Additionally, water scarcity may provoke political unrest, holding the government accountable for bad water management. Governments may be expected to control both water demand and supply. On the one hand, governments can limit water demand by regulating water-intensive industries and establishing water-use policies. On the other hand, they can improve the water supply by investing in water infrastructure. For instance governments can invest in the construction of dams or water reservoirs, waste water management, and in facilitating access to groundwater sources. Therefore, we expect that apart from social disputes, water mass changes are likely to provoke political conflicts, and especially

Table 4: Intensity of conflict

Dependent variable:	**No. of social conflicts**			**No. of casualties**		
Model:	Levels	Log	Poisson	Levels	Log	Poisson
	(1)	(2)	(3)	(4)	(5)	(6)
Δ Water mass	-0.100**	-0.050*	-0.033**	0.967	-0.038	0.003
	(0.049)	(0.027)	(0.016)	(1.268)	(0.061)	(0.004)
Observations	46,752	46,752	46,752	46,752	46,752	46,752
Kleibergen-Paap F stat	28.13	28.13	28.13	28.13	28.13	28.13
Stock-Yogo critcal value (10%)	16.38	16.38	16.38	16.38	16.38	16.38
Fixed effects	Yes	Yes	Yes	Yes	Yes	Yes

Note: The table reports IV coefficient estimates of the number of social conflict and casualties on the change of water mass within each cell. Models include cell and country-year fixed effects. Robust standard errors are clustered at the 3 degree cell level. The means of the dependent variables are 0.03 and 0.52. *** p<0.01, ** p<0.05, * p<0.1

cause unrest targeted towards the government. Water scarcity may also exacerbate already existing grievance, decreasing the opportunity costs to fight and increasing the possibilities of rebel groups to recruit new members. Moreover, rebel groups can strategically damage and capture water infrastructure in order to increase pressure on the population and government, advancing their goals (CNA, 2017). Hence, there is some indication that water mass change also can increase large-scale conflicts.

In order to analyze what types of conflict are caused by water scarcity, we classify the SCAD conflict events into conflict events targeting the state and non-state actors. Second, we analyze resource conflict by focusing on those conflict events that were explicitly listed as arising out of tensions dealing with water, food, subsistence, and environmental degradation in SCAD. Third, we investigate the effects of water declines on organized violence (larger scale conflicts between organized groups, based on the UCDP dataset) and political conflict events (based on the ACLED data). The results are reported in table 5, which shows that the conflict inducing effects of water declines are driven by conflict events targeting the state but not those that are targeting other actors. Civil unrest, demonstrating dissatisfaction with the government, is a major factor driving the effect of water mass change on the likelihood of conflict in our study. Unexpectedly, the results show no significant effect of water mass change on resource conflict. A potential explanation is a lack of power as there are only very few (68) conflicts classified as resource conflict in our database. We find no significant effect of changes in water availability on conflict between organized groups. This result is in contrast to the negative effect found by Couttenier and Soubeyran (2014) using the UCDP data. Yet, it

is important to highlight the distinct definitions of large-scale conflict. Couttenier and Soubeyran (2014) focus on the country-level and on civil wars defined as a year with at least 1000 battle-related deaths, whereas our approach is on the local level and takes also low-intensity organized conflicts into account.

Confirming the role of state actors in the relationship between water availability and conflict, the results show a marginally significant effect of water mass changes on political conflict. With a decrease of 6.7 percentage points in the likelihood of conflict with one further standard deviation increase in water mass change, the magnitude of the effect is comparable to our baseline estimate.

Table 5: Types of conflict

Dependent variable:	**State targeted conflict**	**Non-state targeted conflict**	**Resource conflict**	**Organized conflict**	**Political conflict**
Model:		IV: Second stage			
	(1)	(2)	(3)	(4)	(5)
Δ Water mass	-0.032**	-0.011	-0.007	-0.017	-0.067*
	(0.015)	(0.016)	(0.005)	(0.020)	(0.035)
Dependent variable:			**Δ Water mass**		
Model:			IV: First stage		
Drought months × Δ Global Temp	-0.031***	-0.031***	-0.031***	-0.031***	-0.029***
	(0.006)	(0.006)	(0.006)	(0.006)	(0.006)
Observations	46,752	46,752	46,752	46,752	42,048
Kleibergen-Paap F stat	28.13	28.13	28.13	28.13	21.03
Stock-Yogo critical value (10%)	16.38	16.38	16.38	16.38	16.38
Fixed effects	Yes	Yes	Yes	Yes	Yes

Note: The table reports IV coefficient estimates of distinct types of conflicts on water mass change. State target conflict refers to conflicts targeting the government, and non-state target conflict to all other types of conflict (as reported in SCAD). Resource conflicts are conflicts about water, food, subsistence of environmental degradation (as reported in SCAD). We refer to conflict events reported by UCDP as organized conflict, and to conflict events provided by ACLED as political conflict. All models include cell and country-year fixed effects. Robust standard errors are clustered at the 3 degree grid cell level. *** p<0.01, ** p<0.05, * p<0.1

Previous empirical studies (e.g. Almer et al., 2017; Couttenier and Soubeyran, 2014) focused on Sub-Saharan Africa in their investigation of the effects of droughts on conflict. We expand the geographical range of analysis to increase the external validity of our estimates and include all African countries as well as central America in our sample. Yet, given the differential trends in water mass changes in Africa and central America as shown in figure 2, climate-change-induced droughts may provoke heterogeneous reactions. Additionally, differences in political, economic, cultural, and climatic conditions can determine how to cope with changes in water mass.

In the following, we assess whether the effect is driven by a particular geographical area. We split the sample and estimate our baseline regression model separately for Africa and central America. The estimated coefficients shown in table 6 reveal that the effect is entirely driven by Africa. We find no significant effect for changes in water mass on conflict in central American countries. As a next step, we differentiate Africa into 5 geographical regions and estimate the regression model separately for each region. The results shown in table A1 in the appendix suggest that especially North Africa experienced drought-induced conflicts. This is in line with the descriptive evidence that shows that the Northern region of Africa has the highest number of drought months per year in our sample. However, as the strongly reduced sample size together with saturated fixed effects result in substantially weaker instruments in the regional sub-samples, we consider these results only as indicative.

4.4 Robustness checks

A decrease in rainfall will directly reduce water availability at the surface, but it also has a retarded effect on groundwater recharge and groundwater levels, triggering a groundwater drought (Han et al., 2019). The delay depends on the speed of water movements, which is determined by geological and geographical characteristics (Han et al., 2019). If a population relies mainly on groundwater sources, the retarded effect may have a stronger impact on their behavior than the immediate one. Hence, past water mass change may contribute to conflict, too.

To investigate such temporal dynamics, we include temporal lags of the explanatory variables in our models in table A2. Column 1 shows the baseline regression for the shorter sample period, column 2 includes the first temporal lag of drought months, whereas column 3 includes temporal lags for both drought months and water mass change. The reduction in the sample period only marginally changes the estimated coefficients. A one standard deviation larger water mass reduction increases the likelihood of conflict by 5.4 percentage points as compared to 4.3 percentage points in the main sample (cf. table 2). Column 2 includes the temporal lag of drought months as an additional instrument, whereas in column 3 past water mass change is added to the second stage to measure the delayed effect of water scarcity. In this latter specification, past water mass change is also instrumented. The first stage results for current water mass change in columns 2 and 3 confirm that yearly drought frequency indeed has a cumulative effect on water mass change over time. The duration of drought in the previous year amplifies the decrease in water mass in the current year. The second stage

Table 6: Baseline regression for Africa and central America

Dependent variable:	**Social conflict**			
Model:	IV: Second stage			
Region:	Africa		Central America	
	(1)	(2)	(3)	(4)
Δ Water mass	-0.056**	-0.061**	0.051	0.080
	(0.028)	(0.030)	(0.062)	(0.073)
Temperature		-0.008		0.011
		(0.005)		(0.011)
Meridional wind		-0.001		-0.011
		(0.004)		(0.012)
Zonal wind		-0.001		-0.004*
		(0.001)		(0.002)
Dependent variable:	**Δ Water mass**			
Model:	IV: First stage			
Drought months × Δ Global Temp	-0.029***	-0.027***	-0.046***	-0.043***
	(0.006)	(0.006)	(0.012)	(0.012)
Temperature		-0.134***		-0.074
		(0.031)		(0.045)
Meridional wind		-0.057*		-0.114**
		(0.024)		(0.038)
Zonal wind		0.001		0.020**
		(0.004)		(0.007)
Observations	42,048	42,048	4,656	4,656
Kleibergen-Paap F stat	21.03	18.01	15.45	12.02
Stock-Yogo critical value (10%)	16.38	16.38	16.38	16.38
Fixed effects	Yes	Yes	Yes	Yes

Note: The table reports IV coefficient estimates of the baseline regression model separately for Africa and central America. All models include cell and country-year fixed effects. Robust standard errors are clustered at the 3 degree grid cell level. *** $p<0.01$, ** $p<0.05$, * $p<0.1$

estimates of water mass change on conflict stay of a broadly comparable magnitude throughout all three specifications. In column 3, the temporal lag of water mass change switches sign but is not significant. The weak instrument tests also show F-statistics that lie below the critical values for a 10% potential bias in the IV estimates and indicate that these dynamic results should be interpreted with more caution than our baseline model. Nonetheless, the first and second stage results indicate that droughts have a longer-lasting effect on conflict due to their cumulative effects on water availability. Only current water mass decline seems to induce conflict, while conditional on the current decline, past fluctuations in water availability do not result in more conflict at the present time. Past droughts matter because of their longer lasting effects on water availability, whereas water availability has only an immediate effect on the likelihood of conflict.

Our main results remain qualitatively the same when we change the spatial resolution used in the analysis. Our outcome variable, the incidence of social conflict, and our instrumental variable, the number of drought months combined with global temperature changes, are both measured at a finer resolution and allow for running regressions based on 0.5 degree grid cells, establishing a precise geographical link between local climatic factors and specific conflict events. However, the main explanatory variable, the change in water mass, is only spatially modelled (extrapolated) to a level of 1 degree whereas its precise measurement is based on the 3 degree resolution. We have addressed the spatial interdependence of the changes in water mass that were caused by the higher level of original measurement by clustering the standard errors at the 3 degree level throughout our analyses. This takes into account all potential correlation between the error terms that is induced by measurement errors within the 3-degree grid cell. Alternatively, we re-run the baseline regression on the 0.5 and 3 degree grid-cell resolution to analyze the sensitivity of our estimates to our selection of the spatial resolution. The results are reported in table A3, comparing resolutions of 0.5, 1, and 3 degree grid cells. In all models, we find a negative and significant effect of change in water mass on conflict, validating our main results. The magnitude of the effect increases when we focus on lower levels of resolution and are the largest in the model based on the 3-degree grid, which uses the original native measurement level for water mass changes instead of extrapolated (modelled) outcomes. This indicates that our chosen spatial resolution may result in more measurement error and bias our coefficients downward. We have opted for the 1 degree resolution for our baseline models as they result in more conservative estimates than the more aggregated data and allow us to capture more precisely measured explanatory factors, for instance in the channel

analysis.

Our drought measures are based on SPEI: a multiscalar index that is widely used to measure weather shocks (e.g. Almer et al., 2017; Harari and La Ferrara, 2018). In contrast to the literature that focuses on fluctuations in the average SPEI value, we operationalize droughts by counting the number of months per year in which the SPEI value is below -1. We do so to put a larger emphasis on extreme weather events. We decided to use the threshold of -1 in our main analysis based on the classification of McKee et al. (1993) and Paulo et al. (2012). We test the sensitivity of our estimates by considering other SPEI barriers. In table A4 we present coefficient estimates using the SPEI thresholds of -0.5, -0.75 and -1.5 in addition to our main specification. In the first stage of our IV strategy, weaker thresholds result in a stronger correlation between droughts and water mass change. By contrast, at the second stage, the effect of a drought-induced decline in water mass on conflict is stronger in the specifications that rely on a stricter threshold, suggesting that water mass declines induced by more extreme weather events have a larger capacity to induce conflict.

The exclusion restriction of our instrument may not hold if air pollution is correlated with conflict and droughts. Rosenfeld (2000) shows that air pollution, especially aerosols, can shut-off precipitation. Even though there is no evidence of a direct effect of air pollution on conflict, an indirect effect via economic development or population growth is probable. Therefore, we test the robustness of our results by controlling for air pollution. Table A5 reports the regression results. In column 1 we show the baseline estimate for the reduced sample, column 2 reports estimates of our baseline model including particulate matter of size equal or smaller than 2.5 microns as a control, and in column 3 PM 2.5 density enters the regression in the form of the inverse hyperbolic sine function.[8] Our main result is robust to the inclusion of any functional form of PM 2.5 density. Referring to column 2, we see a positive correlation between air pollution and conflict.

In our main analysis we include cell and country-year fixed effects to account for potential endogeneity biases. However, this may absorb too much of the spatio-temporal variation, especially if the strength of drought shocks varies mostly across but not within countries. As a comparison, we also provide alternative, less restrictive regression models to assess the sensitivity of our results to model specification. In table A6, we replace the country-year with year fixed effects only in column 1 and exchange them with country specific time trends in columns 2 to 4. Column 3 includes the climatic con-

[8] We use data from the global gridded dataset on PM 2.5 density provided by van Donkelaar et al. (2018). Data are available for the years 2002–2016. Hence we lack one year.

trols and year fixed effects as well. The model in column 4 includes a quadratic time trend instead of a linear one. The estimated effect size from water mass change on social conflict is somewhat lower in these less restrictive models whereas our instrument gains in strength in these specifications. In all model specifications, water mass change is still statistically significantly negatively related to the likelihood of social conflict, confirming the general robustness of our main results.

5 Conclusion

Due to the ongoing climate change and a globally rising demand for water, the consequences of water scarcity have been gaining policy importance. In this paper, we assess the effects of changing water availability on conflict at the local level. In a cell-year panel covering Africa, central America, and the Caribbean over the years of 2002 to 2017, we estimate the effect of changes in the total available water mass on the likelihood of conflict. We combine novel satellite data on water mass movements, provided by the Gravity Recovery and Climate Experiment (GRACE) mission from US and German space agencies (NASA and DLR), with social conflict events from the Social Conflict Analysis Database (SCAD). In order to establish a causal effect of water mass change on conflict, we implement an instrumental variable approach, instrumenting changes in total water mass by the number of drought months per year interacted with yearly changes in the global average temperature.

Our estimates reveal the total effect of a reduction in local water mass on conflict, resulting from rainfall shocks, less runoff but also groundwater depletion. Thus, we contribute to the literature by not only focusing on the effects of drought shocks in a reduced form, but linking social conflicts to their true driver, the worsening access to water that is a vital natural resource. Moreover, in contrast to the previous literature, we focus on the effect of global-warming induced changes in the water cycle on conflict. We thereby follow the suggestion by Couttenier and Soubeyran (2014) to focus on aggregate shocks.

Our results show that a reduction in total water mass increases the likelihood of conflict. A one standard deviation larger decrease in water mass more than triples the likelihood of local conflict, which is a substantial effect. We find considerable heterogeneity in the effects by water supply factors. Acting as a buffer, access to groundwater and the availability of surface water reduces the effect of water mass change on conflict substantially. This is in line with the results by Almer et al. (2017). When assessing

the role of demand factors, we are able to further refine the results by Almer et al. (2017) and Harari and La Ferrara (2018) by showing that excess water demand leads to a quicker depletion of water resources in case of drought shocks, which generates more conflict. The higher water demand amplifies the negative effects of droughts on local water mass and hence, drought shocks disproportionately increase the likelihood of water scarcity in areas with a high water demand. Yet, the effect of increasing resource scarcity results in the same increase in the probability of conflict in places with relatively higher or lower water demand. Moreover, the results indicate that studies focusing on the effects of contemporaneous droughts tend to underestimate the scope of their effects as local water availability responds strongly not only to current but also to past droughts.

Our results highlight that governments' water resource management strategies play a crucial role not only for climate change adaptation but also for reducing the local potential of social conflict. Facilitating access to groundwater can reduce the susceptibility to variations in rainfall, also reducing the occurrence of localized social conflict.

References

AghaKouchak, Amir, Ali Mirchi, Kaveh Madani, Giuliano Di Baldassarre, Ali Nazemi, Aneseh Alborzi, Hassan Anjileli, Marzi Azarderakhsh, Felicia Chiang, Elmira Hassanzadeh et al., "Anthropogenic Drought: Definition, Challenges, and Opportunities," *Review of Geophysics*, 2021, (2).

Allan, Richard P, "The role of water vapour in Earth's energy flows," *Surveys in Geophysics*, 2012, *33* (3-4), 557–564.

Almås, Ingvild, Maximilian Auffhammer, Tessa Bold, Ian Bolliger, Aluma Dembo, Solomon M Hsiang, Shuhei Kitamura, Edward Miguel, and Robert Pickmans, "Destructive behavior, judgment, and economic decision-making under thermal stress," Working paper, National Bureau of Economic Research 2019.

Almer, Christian, Jérémy Laurent-Lucchetti, and Manuel Oechslin, "Water scarcity and rioting: Disaggregated evidence from Sub-Saharan Africa," *Journal of Environmental Economics and Management*, 2017, *86*, 193–209.

Anderson, Craig A, "Temperature and aggression: ubiquitous effects of heat on occurrence of human violence.," *Psychological Bulletin*, 1989, *106* (1), 74.

_ , Kathryn B Anderson, Nancy Dorr, Kristina M DeNeve, and Mindy Flanagan, "Temperature and aggression," *Advances in Experimental Social Psychology*, 2000, *32*, 63–133.

Balk, Deborah L, Uwe Deichmann, Greg Yetman, Francesca Pozzi, Simon I Hay, and Andy Nelson, "Determining global population distribution: methods, applications and data," *Advances in Parasitology*, 2006, *62*, 119–156.

Breckner, Miriam and Uwe Sunde, "Temperature extremes, global warming, and armed conflict: new insights from high resolution data," *World Development*, 2019, *123*, 104624.

Brückner, Markus, "Population size and civil conflict risk: is there a causal link?," *The Economic Journal*, 2010, *120* (544), 535–550.

Brutsaert, Wilfried, "Global land surface evaporation trend during the past half century: Corroboration by Clausius-Clapeyron scaling," *Advances in Water Resources*, 2017, *106*, 3–5.

Burke, Marshall, Solomon M Hsiang, and Edward Miguel, "Climate and conflict," *Annual Review of Economics*, 2015, *7*, 577–617.

Chambers, Don P and Jennifer A Bonin, "Evaluation of Release-05 GRACE time-variable gravity coefficients over the ocean," *Ocean Science*, 2012, *8* (5), 859.

Ciccone, Antonio, "Economic shocks and civil conflict: A comment," *American Economic Journal: Applied Economics*, 2011, *3* (4), 215–27.

CNA, "The role of water stress in instability and conflict," 2017. Final report CRM-2017-U-016532 of the CNA Military Advisory Board.

Cooley, Savannah S. and Felix W. Landerer, "Gravity Recovery and Climate Experiment (GRACE) Follow-On (GRACE-FO) Level-3 Data Product User Handbook," 2019.

Couttenier, Mathieu and Raphael Soubeyran, "Drought and civil war in Sub-Saharan Africa," *The Economic Journal*, 2014, *124* (575), 201–244.

Croicu, Mihai and Ralph Sundberg, "UCDP georeferenced event dataset codebook version 4.0," *Journal of Peace Research*, 2015, *50* (4), 523–532.

Dell, Melissa, Benjamin F Jones, and Benjamin A Olken, "What do we learn from the weather? The new climate-economy literature," *Journal of Economic Literature*, 2014, *52* (3), 740–98.

Dessler, AE, Z Zhang, and P Yang, "Water-vapor climate feedback inferred from climate fluctuations, 2003–2008," *Geophysical Research Letters*, 2008, *35* (20).

Döring, Stefan, "Come rain, or come wells: How access to groundwater affects communal violence," *Political Geography*, 2020, *76*, 102073.

Dube, Oeindrila and Juan F Vargas, "Commodity price shocks and civil conflict: Evidence from Colombia," *The Review of Economic Studies*, 2013, *80* (4), 1384–1421.

Fan, Ying, H Li, and Gonzalo Miguez-Macho, "Global patterns of groundwater table depth," *Science*, 2013, *339* (6122), 940–943.

Garner, R, T Naidu, C Saavedra, P Matamoros, and E Lacroix, "Water Management in Mining: A Selection of Case Studies," *International Council on Mining & Metals, London*, 2012.

Gatti, Nicolas, Kathy Baylis, and Benjamin Crost, "Can irrigation infrastructure mitigate the effect of rainfall shocks on conflict? Evidence from Indonesia," *American Journal of Agricultural Economics*, 2021, *103* (1), 211–231.

Han, Shin-Chan, Che-Kwan Shum, Michael Bevis, Chen Ji, and Chung-Yen Kuo, "Crustal dilatation observed by GRACE after the 2004 Sumatra-Andaman earthquake," *Science*, 2006, *313* (5787), 658–662.

Han, Zhiming, Shengzhi Huang, Qiang Huang, Guoyong Leng, Hao Wang, Qingjun Bai, Jing Zhao, Lan Ma, Lu Wang, and Meng Du, "Propagation dynamics from meteorological to groundwater drought and their possible influence factors," *Journal of Hydrology*, 2019, *578*, 124102.

Harari, Mariaflavia and Eliana La Ferrara, "Conflict, climate, and cells: a disaggregated analysis," *Review of Economics and Statistics*, 2018, *100* (4), 594–608.

Hodler, Roland and Paul A Raschky, "Economic shocks and civil conflict at the regional level," *Economics Letters*, 2014, *124* (3), 530–533.

Homer-Dixon, Thomas F, "Environmental scarcities and violent conflict: evidence from cases," *International Security*, 1994, *19* (1), 5–40.

Hsiang, Solomon M, Marshall Burke, and Edward Miguel, "Quantifying the influence of climate on human conflict," *Science*, 2013, *341* (6151).

Huntington, Thomas G, "Evidence for intensification of the global water cycle: Review and synthesis," *Journal of Hydrology*, 2006, *319* (1-4), 83–95.

_ , "Climate warming-induced intensification of the hydrologic cycle: an assessment of the published record and potential impacts on agriculture," *Advances in Agronomy*, 2010, *109*, 1–53.

Kalnay, Eugenia, Masao Kanamitsu, Robert Kistler, William Collins, Dennis Deaven, Lev Gandin, Mark Iredell, Suranjana Saha, Glenn White, John Woollen et al., "The NCEP/NCAR 40-year reanalysis project," *Bulletin of the American Meteorological Society*, 1996, *77* (3), 437–472.

Klosko, S, D Rowlands, S Luthcke, F Lemoine, D Chinn, and M Rodell, "Evaluation and validation of mascon recovery using GRACE KBRR data with independent mass flux estimates in the Mississippi Basin," *Journal of Geodesy*, 2009, *83* (9), 817–827.

Kuchment, Lev S, "The hydrological cycle and human impact on it," *Water Resources Management*, 2004, p. 40.

Landerer, FW, FM Flechtner, H Save, FH Webb, T Bandikova, WI Bertiger, SV Bettadpur, S Byun, C Dahle, H Dobslaw et al., "Extending the global mass change data record: GRACE Follow-On instrument and science data performance," *Geophysical Research Letters*, 2020, *47*, e2020GL088306.

Maus, Victor, Stefan Giljum, Jakob Gutschlhofer, Dieison M da Silva, Michael Probst, Sidnei LB Gass, Sebastian Luckeneder, Mirko Lieber, and Ian McCallum, "A global-scale data set of mining areas," *Scientific Data*, 2020, *7* (1), 1–13.

McKee, Thomas B, Nolan J Doesken, and John Kleist, "The relationship of drought frequency and duration to time scales," *Proceedings of the 8th Conference on Applied Climatology*, 1993, *17* (22), 179–183.

Miguel, Edward, Shanker Satyanath, and Ernest Sergenti, "Economic shocks and civil conflict: An instrumental variables approach," *Journal of Political Economy*, 2004, *112* (4), 725–753.

Milrad, Shawn, *Synoptic Analysis and Forecasting: An Introductory Toolkit*, Elsevier, 2017.

Natural Earth, "River and lake centerlines," Dataset, Natural Earth 2020. available at https://www.naturalearthdata.com/downloads/10m-physical-vectors/10m-rivers-lake-centerlines/, [accessed on 30.9.2020].

Nelson, Travis, "When disaster strikes: on the relationship between natural disaster and interstate conflict," *Global Change, Peace & Security*, 2010, *22* (2), 155–174.

Oki, Taikan and Shinjiro Kanae, "Global hydrological cycles and world water resources," *Science*, 2006, *313* (5790), 1068–1072.

Otto, Betsy and Leah Schleifer, "Domestic water use grew over 600 percent over the past 50 years," Webpage, World Resource Institute 2020. https://www.wri.org/blog/2020/02/growth-domestic-water-use, [accessed 16.07.2020].

Pan, Shufen, Hanqin Tian, Shree RS Dangal, Qichun Yang, Jia Yang, Chaoqun Lu, Bo Tao, Wei Ren, and Zhiyun Ouyang, "Responses of global terrestrial evapotranspiration to climate change and increasing atmospheric CO2 in the 21st century," *Earth's Future*, 2015, *3* (1), 15–35.

Paulo, AA, RD Rosa, and LS Pereira, "Climate trends and behaviour of drought indices based on precipitation and evapotranspiration in Portugal," *Natural Hazards and Earth System Sciences*, 2012, *12* (5), 1481–1491.

Raleigh, Clionadh, Andrew Linke, Håvard Hegre, and Joakim Karlsen, "Introducing ACLED: an armed conflict location and event dataset: special data feature," *Journal of Peace Research*, 2010, *47* (5), 651–660.

Richards, Alan and Nirvikar Singh, "Inter-state water disputes in India: Institutions and policies," *International Journal of Water Resources Development*, 2002, *18* (4), 611–625.

Richts, A, W Struckmeier, and M Zaepke, "WHYMAP and the Groundwater Resources of the World 1: 25,000,000 Sustaining Groundwater Resources, International Year of Planet Earth ed J Jones," 2011.

Rosenfeld, Daniel, "Suppression of rain and snow by urban and industrial air pollution," *Science*, 2000, *287* (5459), 1793–1796.

Salehyan, Idean, Cullen S Hendrix, Jesse Hamner, Christina Case, Christopher Linebarger, Emily Stull, and Jennifer Williams, "Social conflict in Africa: A new database," *International Interactions*, 2012, *38* (4), 503–511.

Sarsons, Heather, "Rainfall and conflict: A cautionary tale," *Journal of Development Economics*, 2015, *115*, 62–72.

Sasgen, Ingo, Bert Wouters, Alex S Gardner, Michalea D King, Marco Tedesco, Felix W Landerer, Christoph Dahle, Himanshu Save, and Xavier Fettweis, "Return to rapid ice loss in Greenland and record loss in 2019 detected by the GRACE-FO satellites," *Communications Earth & Environment*, 2020, *1* (1), 1–8.

Scanlon, Bridget R, Zizhan Zhang, Himanshu Save, David N Wiese, Felix W Landerer, Di Long, Laurent Longuevergne, and Jianli Chen, "Global evaluation of new GRACE mascon products for hydrologic applications," *Water Resources Research*, 2016, *52* (12), 9412–9429.

Scheffran, Jürgen, Michael Brzoska, Jasmin Kominek, PMichael Link, Janpeter Schilling et al., "Climate change and violent conflict," *Science*, 2012, *336* (6083), 869–871.

Schulz, Klaus J and Joseph A Briskey, "Major mineral deposits of the world," Dataset, US Geological Survey 2005. available at https://mrdata.usgs.gov/major-deposits, [accessed on 15.04.2020].

SEDAC, "Global Rural-Urban Mapping Project, Version 1 (GRUMPv1): Urban Extents Grid," Dataset, NASA Socioeconomic Data and Applications Center (SEDAC), Center for International Earth Science Information Network (CIESIN), International Food Policy Research Institute (IFPRI), The World Bank, and Centro Internacional de Agricultura Tropical (CIAT) 2011. available at https://sedac.ciesin.columbia.edu/data/set/grump-v1-urban-extents, [accessed on 15.10.2020].

Siebert, Stefan, Verena Henrich, Karen Frenken, and Jacob Burke, "Update of the digital global map of irrigation areas to version 5," *Rheinische Friedrich-Wilhelms-Universität, Bonn, Germany and Food and Agriculture Organization of the United Nations, Rome, Italy*, 2013.

Skliris, Nikolaos, Jan D Zika, George Nurser, Simon A Josey, and Robert Marsh, "Global water cycle amplifying at less than the Clausius-Clapeyron rate," *Scientific Reports*, 2016, *6* (1), 1–9.

Slettebak, Rune T, "Don't blame the weather! Climate-related natural disasters and civil conflict," *Journal of Peace Research*, 2012, *49* (1), 163–176.

Theisen, Ole Magnus, Nils Petter Gleditsch, and Halvard Buhaug, "Is climate change a driver of armed conflict?," *Climatic Change*, 2013, *117* (3), 613–625.

Thenkabail, Prasad S, Chandrashekhar M Biradar, Praveen Noojipady, Venkateswarlu Dheeravath, Yuanjie Li, Manohar Velpuri, Muralikrishna Gumma, Obi Reddy P Gangalakunta, Hugh Turral, Xueliang Cai et al., "Global irrigated area map (GIAM), derived from remote sensing, for the end of the last millennium," *International Journal of Remote Sensing*, 2009, *30* (14), 3679–3733.

van Donkelaar, Aaron, Randall V Martin, Michael Brauer, N Christina Hsu, Ralph A Kahn, Robert C Levy, Alexei Lyapustin, Andrew M Sayer, and David M Winker, "Documentation for the Global Annual PM2. 5 Grids from MODIS, MISR and SeaWiFS Aerosol Optical Depth (AOD) with GWR, 1998-2016," *Palisades NY: NASA Socioeconomic Data and Applications Center*, 2018.

Vicente-Serrano, Sergio M, Santiago Beguería, and Juan I López-Moreno, "A multiscalar drought index sensitive to global warming: The standardized precipitation evapotranspiration index," *Journal of Climate*, 2010, *23* (7), 1696–1718.

Viron, O De, I Panet, V Mikhailov, M Van Camp, and M Diament, "Retrieving earthquake signature in grace gravity solutions," *Geophysical Journal International*, 2008, *174* (1), 14–20.

Vörösmarty, Charles J and Dork Sahagian, "Anthropogenic disturbance of the terrestrial water cycle," *Bioscience*, 2000, *50* (9), 753–765.

Waliser, Duane and Bin Guan, "Extreme winds and precipitation during landfall of atmospheric rivers," *Nature Geoscience*, 2017, *10* (3), 179–183.

Watkins, Michael M, David N Wiese, Dah-Ning Yuan, Carmen Boening, and Felix W Landerer, "Improved methods for observing Earth's time variable mass distribution with GRACE using spherical cap mascons," *Journal of Geophysical Research: Solid Earth*, 2015, *120* (4), 2648–2671.

Wiese, D. N., D.-N. Yuan, C. Boening, F. W. Landerer, and M. M. Watkins, "JPL GRACE mascon ocean, ice, and hydrology equivalent water height release 06 Coastal Resolution Improvement (CRI) filtered version 1.0. Ver. 1.0.," Technical Report, Physical Oceanography Distributed Active Archive Center (PO:DAAC), CA, USA 2018. http://dx.doi.org/10.5067/TEMSC-3MJC6.

Wiese, David N, Felix W Landerer, and Michael M Watkins, "Quantifying and reducing leakage errors in the JPL RL05M GRACE mascon solution," *Water Resources Research*, 2016, *52* (9), 7490–7502.

World Economic Forum, "Water scarcity is one of the greatest challenges of our time," Webpage, World Economic Forum 2020. https://www.weforum.org/agenda/2019/03/water-scarcity-one-of-the-greatest-challenges-of-our-time, [accessed on 24.02.2020].

Xu, Jiuping, Ziqi Wang, Feng Shen, Chi Ouyang, and Yan Tu, "Natural disasters and social conflict: A systematic literature review," *International Journal of Disaster Risk Reduction*, 2016, *17*, 38–48.

6 Appendix

Table A1: Heterogenous effects within Africa

Dependent variable:	**Social conflict**				
Model:	IV: Second stage				
Africa region:	North	South	East	West	Central
	(1)	(2)	(3)	(4)	(5)
Δ Water mass	-0.200***	-0.014	0.003	0.020	-0.226
	(0.064)	(0.029)	(0.118)	(0.059)	(0.329)
Dependent variable:	Δ **Water mass**				
Model:	IV: First stage				
Drought months $\times$ Δ Global temp	-0.021***	-0.036	-0.018	-0.048***	-0.013
	(0.006)	(0.022)	(0.012)	(0.010)	(0.016)
Observations	11,552	8,640	6,992	8,576	3,520
Kleibergen-Paap F stat	12.52	2.734	2.418	21.81	0.666
Stock-Yogo critical value (10%)	16.38	16.38	16.38	16.38	16.38
Fixed effects	Yes	Yes	Yes	Yes	Yes

Note: The table reports IV coefficient estimates of the baseline regression model separately for regions within Africa. All models include cell and country-year fixed effects. Robust standard errors are clustered at the 3 degree grid cell level. *** p<0.01, ** p<0.05, * p<0.1

Table A2: Time dynamics

Dependent variable:	**Social conflict**		
Model:	IV: Second stage		
	(1)	(2)	(3)
Δ Water mass	-0.054*	-0.035	-0.043*
	(0.028)	(0.023)	(0.024)
Δ Water mass$_{t-1}$			0.035
			(0.022)
Dependent variable:	Δ **Water mass**		
Model:	IV: First stage		
Drought months $\times$ Δ Global temp	-0.028***	-0.025***	-0.025***
	(0.006)	(0.006)	(0.006)
(Drought months $\times$ Δ Global temp)$_{t-1}$		-0.018***	-0.018***
		(0.005)	(0.005)
Dependent variable:	Δ **Water mass**$_{t-1}$		
Model:	IV: First stage		
Drought months $\times$ Δ Global temp			0.015*
			(0.006)
(Drought months $\times$ Δ Global temp)$_{t-1}$			-0.031***
			(0.006)
Observations	43,830	43,830	43,830
Kleibergen-Paap F stat	19.79	11.02	8.857
Stock-Yogo critical value (10%)	16.38	19.93	7.03
Fixed effects	Yes	Yes	Yes

Note: The table reports IV coefficient estimates of social conflict on present and past changes in water mass at the cell level. Water mass change is instrumented by the number of past and present drought months. All models include cell and country-year fixed effects. Robust standard errors are clustered at the 3 degree grid cell level. *** p<0.01, ** p<0.05, * p<0.1

Table A3: Robustness: level of observation

Dependent variable:	**Social conflict**		
	(1)	(2)	(3)
Model:	IV: Second stage		
Level of obs.:	0.5 °	1 °	3 °
Δ Water mass	-0.064*	-0.043*	-0.267**
	(0.003)	(0.024)	(0.095)
	Δ Water mass		
	IV: First stage		
Drought months × Δ Global temp	-0.007***	-0.031***	-0.053***
	(0.001)	(0.006)	(0.010)
Observations	177,200	46,752	6,016
Kleibergen-Paap F-stat	28.06	28.13	27.94
Stock-Yogo critical value (10%)	16.38	16.38	16.38
Fixed effects	Yes	Yes	Yes
Mean dependent variable	0.01	0.02	0.14

Note: The table reports IV coefficient estimates of social conflict on changes in water mass at different cell levels. Water mass change is instrumented by the number of drought months. All models include cell and country-year fixed effects. Robust standard errors are clustered at the 3 degree grid cell level. *** p<0.01, ** p<0.05, * p<0.1

Table A4: Alternative drought specifications

Dependent variable:	**Social conflict**			
Model:	IV: Second stage			
SPEI threshold:	-0.5	-0.75	-1	-1.5
	(1)	(2)	(3)	(4)
Δ Water mass	-0.005	-0.033*	-0.043*	-0.104**
	(0.015)	(0.019)	(0.024)	(0.045)
Dependent variable:	Δ Water mass			
Model:	IV: First stage			
Drought months × Δ Global temp	-0.042***	-0.036***	-0.031***	-0.024***
	(0.006)	(0.006)	(0.006)	(0.007)
Observations	46,752	46,752	46,752	46,752
Kleibergen-Paap F stat	44.20	35.27	28.13	11.14
Stock-Yogo critical value (10%)	16.38	16.38	16.38	16.38
Fixed effects	Yes	Yes	Yes	Yes

Note: The table reports IV coefficient estimates of social conflict on changes in water mass with alternative drought definitions as indicated in the table. Water mass change is instrumented by the number of drought months. All models include cell and country-year fixed effects. Robust standard errors are clustered at the 3 degree grid cell level. *** $p<0.01$, ** $p<0.05$, * $p<0.1$

Table A5: Controlling for air pollution

Dependent variable:	**Social conflict**		
Model:	IV: Second stage		
	(1)	(2)	(3)
Δ Water mass	-0.059**	-0.057*	-0.056*
	(0.030)	(0.034)	(0.034)
PM 2.5 density		0.003*	
		(0.001)	
PM 2.5 density (asinh)			0.010
			(0.009)
Dependent variable:	**Δ Water mass**		
Model:	IV: First stage		
Drought months × Δ Global temp	-0.028***	-0.026***	-0.026***
	(0.007)	(0.007)	(0.007)
PM 2.5 density		0.009	
		(0.018)	
PM 2.5 density (asinh)			-0.045
			(0.101)
Observations	43,830	38,505	38,505
Kleibergen-Paap F stat	17.47	13.40	13.47
Stock-Yogo critical value (10%)	16.38	16.38	16.38
Fixed effects	Yes	Yes	Yes

Note: The table reports IV coefficient estimates of social conflict on changes in water mass controlling for PM 2.5 density. The regressions include cell and country-year fixed effects. Water mass change is instrumented by the number of drought months. Robust standard errors are clustered at the 3 degree grid cell level. *** p<0.01, ** p<0.05, * p<0.1

Table A6: Alternative regression models

Dependent variable:	**Social conflict**			
Model:	IV: Second stage			
	(1)	(2)	(3)	(4)
Δ Water mass	-0.017**	-0.015*	-0.025**	-0.025**
	(0.008)	(0.008)	(0.012)	(0.012)
Temperature			-0.004	-0.004
			(0.004)	(0.004)
Meridional wind			0.002	0.002
			(0.002)	(0.002)
Zonal wind			-0.000	-0.000
			(0.000)	(0.000)
Dependent variable:	**Δ Water mass**			
Model:	IV: First stage			
Drought months × Δ Global temp	-0.072***	-0.071***	-0.051***	-0.051***
	(0.010)	(0.008)	(0.007)	(0.007)
Temperature			-0.236***	-0.236***
			(0.028)	(0.028)
Meridional wind			0.012	0.012
			(0.010)	(0.010)
Zonal wind			0.003	0.003
			(0.002)	(0.002)
Observations	46,752	46,752	46,752	46,752
Cell FE	Yes	Yes	Yes	Yes
Year FE	Yes		Yes	Yes
Country time trend		Yes	Yes	
Squared country time trend				Yes
Kleibergen-Paap F stat	57.03	76.58	53.81	53.79
Stock-Yogo critical value (10%)	16.38	16.38	16.38	16.38

Note: The table reports IV coefficient estimates of social conflict on changes in water mass with alternative fixed effects specifications indicated in the table. Water mass change is instrumented by the number of drought months. All models include cell and country-year fixed effects. Robust standard errors are clustered at the 3 degree grid cell level. *** p<0.01, ** p<0.05, * p<0.1

Table A7: Variable definitions

Dependent and main variables	
Social conflict	Indicator variable that takes one if in the respective year and cell a conflict event occurred, based on the SCAD conflict dataset (Salehyan et al., 2012).
No. of social conflicts	Number of conflict events that occurred in year t in cell c, based on the SCAD conflict dataset (Salehyan et al., 2012).
No. of casualties	Number of battle-related casualties that occurred in year t in cell c, based on the SCAD conflict dataset (Salehyan et al., 2012).
State target conflict	Indicator variable that takes one if in the respective year and cell a conflict event occurred that was targeted towards the government, based on the SCAD dataset (Salehyan et al., 2012).
Non-state target conflict	Indicator variable that takes one in the respective year and cell a conflict event occurred that was not targeted towards the government, based on the SCAD conflict dataset (Salehyan et al., 2012).
Resource conflict	Indicator variable that takes one if in the respective year and cell a conflict event occurred that was triggered mainly by a natural resource issue. A resource conflict is defined as a conflict were the first, second or third mentioned issue of tension is classified as food, water, subsistence or environmental degradation. Source: Salehyan et al. (2012)
Organized conflict	Indicator variable that takes one if in the respective year and cell a conflict event occurred reported by the UCDP datset. Source: UCDP
Political conflict	Indicator variable that takes one if in the respective year and cell a conflict event occurred reported by the ACLED datset. Source: ACLED
Drought months	Records the number of drought months per year and cell. A drought month is defined as a month with SPEI values below -1. Source: Vicente-Serrano et al. (2010).
Δ Global temp	gives the yearly average change in global temperature. Source: GHCN-M and ICOADS.
Demand and supply factors	
Surface water	Indicator variable that takes one if a river or lake is located in the respective grid. Source: Natural Earth
Groundwater access	Indicator variable that takes one if groundwater is accessible. We define access by low depth to groundwater (below median) and high groundwater storage. Source: Fan et al. (2013) and WHYMAP from BGR
Irrigation	Indicator variable that takes one if irrigated areas are located in the cell. Source: GIAM .
Mining	Indicator variable that takes one if in the cell a major mineral deposit or a mineral extraction site is located. Source: Schulz and Briskey (2005) and Maus et al. (2020).
Urbanization	gives the share of urban areas located in the grid. Source: SEDAC.

Control variables	
Temperature	Gives temperature anomalies in degree Celsius of a year in a cell. Source: Kalnay et al. (1996).
Meridional velocity	Gives the demeaned average wind speed in meter per second of a year in a cell from north to south. Source: Kalnay et al. (1996).
Zonal velocity	Gives the demeaned average wind speed in meter per second of a year in a cell from east to west. Source: Kalnay et al. (1996).
Robustness checks	
PM 2.5 density	Gives the average particulate matter of size equal and smaller than 2.5 microns density in the air on the 1 degree grid cell level. Source: van Donkelaar et al. (2018).